A specific *ovarian tumor* protein isoform is required for efficient differentiation of germ cells in *Drosophila* oogenesis

Wayne R. Steinhauer[1] and Laura J. Kalfayan

Department of Biochemistry and Biophysics, The University of North Carolina at Chapel Hill, Chapel Hill, North Carolina 27599 USA

Mutations within the *ovarian tumor* (*otu*) gene result in abnormal ovarian development. It has been proposed that *otu* phenotypes result from abnormal germ cell division and differentiation. To understand better what role *otu* performs in oogenesis we have undertaken an analysis of protein expression from the *otu* locus. Anti-*otu* antibodies recognize two proteins from *Drosophila* ovary extracts with apparent molecular masses of 98 and 104 kD. Sequence analysis of *otu* cDNAs suggests that these proteins are translated from two mRNAs generated by alternative splicing of a 126-bp exon between the sixth and seventh exon of the smaller transcript. Analysis of *otu* protein expression in eight mutants indicates a correlation between the accumulation of the 104-kD isoform and predifferentiated germ cells and suggests that there is a developmental shift in the accumulation of the two isoforms upon differentiation of germ cells. Furthermore, the 104-kD isoform appears to be required for efficient differentiation of germ cells. Immunostaining of *otu* proteins is restricted to the cytoplasm of germ cells, and a rapid loss of oocyte immunostaining during stage 11 suggests that there is a rapid and selective degradation of *otu* proteins within the oocyte but not within its 15 interconnected nurse cells.

[*Key Words*: *ovarian tumor*; oogenesis; alternative splicing; developmental regulation; differentiation]

Received September 4, 1991; revised version accepted December 13, 1991.

Drosophila has evolved a highly efficient means of synthesizing the large quantities of mRNA and protein required in early embryogenesis prior to the onset of zygotic transcription. The adaptation involves the generation of an egg chamber consisting of an oocyte and 15 germ-line-derived nurse cells that are connected to one another by cytoplasmic bridges. The nurse cells perform a trophic function, that is, their polyploidization dramatically increases the synthetic capacity within the egg chamber. The basic structure of an egg chamber is laid down in the germarium: The daughter of a stem cell (a cystoblast) proceeds through 4 successive and incomplete mitotic divisions to generate a 16 cell cyst, which is then surrounded by a layer of somatically derived follicle cells. The 16 cells or cystocytes are connected in a specific arrangement by structures termed ring canals (King et al. 1956; Brown and King 1964; Kinderman and King 1973); one cystocyte will develop as an oocyte, and the remaining 15 differentiate as nurse cells. Before the egg chamber leaves the germarium and enters the vitellarium, mitotic germ cell division within the egg chamber ceases and differentiation of cystocytes is initiated.

The development of the egg chamber toward a mature egg as it progresses along the vitellarium has been subdivided into 14 morphological stages (King et al. 1956; Cummings and King 1969; Mahowald and Kambysellis 1980). In the previtellogenic stages (1–7), the nurse cells undergo many rounds of endomitotic DNA replication and actively synthesize RNA and proteins that are transported to the oocyte through the ring canals (King 1970; Mahowald and Kambysellis 1980; Mulligan and Rasch 1985). In the vitellogenic stages (8–14), the oocyte increases rapidly in size. A significant portion of this increase is contributed by nurse cells, which continue to increase in size through stage 10 and then rapidly transfer their cytoplasm to the oocyte during stage 11. In the final stages of oogenesis, nurse cell nuclei degenerate and somatically derived follicle cells complete the formation of the egg membranes and their associated structures.

Thus, oogenesis entails a highly specialized pattern of cell divisions and the differentiation of cystocytes along the different developmental pathways of nurse cells and oocytes. To understand better how these processes are controlled, we have undertaken a molecular analysis of the *ovarian tumor* (*otu*) gene, mutations of which disrupt these processes. The *otu* gene is a potentially promising candidate for a molecular analysis of oogenesis, because *otu* mutants display a remarkable range of ovarian

[1]**Present address: Laboratory of Genetics, National Institute of Environmental Health Sciences, Research Triangle Park, North Carolina 27709 USA.**

pathologies. Seventeen ethylmethane sulfonate (EMS)-induced, and 13 P-element-induced, or P-element-derived, *otu* mutants have been recovered (Gans et al. 1975; Mohler 1977; Digan 1980; King and Riley 1982; King et al. 1986; Mulligan et al. 1988; G. Sass and D. Mohler, unpubl.). The phenotypes displayed by *otu* mutants are divided into three developmental classes that highlight specific steps within oogenesis which may be affected by or under the control of the *otu* gene (King et al. 1986). An *otu* mutant is classified by the predominant phenotype displayed within the ovary; however, multiple phenotypes may be present in any given ovary.

The quiescent (QUI) class is the most severe and represents mutants in which germ cells fail to proliferate, causing ovarioles to appear as empty sheaths of somatic tissue (King and Riley 1982). Mutants from the oncogenic (ONC) class have lost the ability to control cystocyte divisions: the usual four incomplete rounds of mitosis are replaced by complete and continued cell divisions, giving rise to tumorous egg chambers filled with hundreds of undifferentiated cystocytes (King 1979). The differentiated (DIF) class encompasses mutants with ovaries that predominantly contain egg chambers exhibiting some form of differentiation. Cystocyte divisions are not always precise, and some alleles exhibit odd numbers of nurse cells or no oocyte. Those egg chambers that contain oocytes usually proceed through oogenesis to what has been called a "pseudo-12" (p12) stage but do not complete development (King et al. 1986; Storto and King 1988).

Initial molecular characterization of the *otu* gene and its products identified a predominant 3.2-kb ovary-specific transcript (Mulligan et al. 1988). Sequence analysis suggested that *otu* generated a single 811-amino-acid protein with a 12% proline content. Here, we describe a second *otu* protein isoform expressed in ovaries that is generated through alternative splicing and examine alterations in expression of the two isoforms in eight *otu* mutants. Our results suggest that a specific isoform is required for efficient differentiation of the germ cells and that differentiation may bring about a shift in the expression of the two protein isoforms. Immunolocalization of *otu* proteins in situ suggests that *otu* is a germ cell-specific cytoplasmic protein and that its expression is differentially regulated between nurse cells and oocytes through a rapid and selective degradation of *otu* protein within the oocyte at stage 11.

Results

Two protein isoforms are evident from analysis of otu *gene products*

Previous sequence analysis of the *otu* gene and several *otu* cDNAs suggested that *otu* produced a single protein of 811 amino acids (Steinhauer et al. 1989). We raised polyclonal antibodies that recognize two specific regions of this *otu* gene product: amino acids 253–671 and 670–811. Coding regions used in *lacZ–otu* fusion constructs are shown below a schematic representation of an *otu* cDNA (Fig. 1A). The unmodified expression vector (pWR590) produces a truncated form of β-galactosidase with a molecular mass of ~80 kD (Fig. 2, lane 2), whereas fusion proteins produced from constructs 1 and 2 have masses of ~140 and 90 kD, respectively (Fig. 2, lanes 3,4).

Rabbit polyclonal antibodies against the two domains of *otu* protein were purified on fusion protein-affinity columns to generate anti-*otu*(253–671)- and anti-*otu*(670–811)-specific antisera. Antisera specificities were examined in *Escherichia coli* extracts and in crude

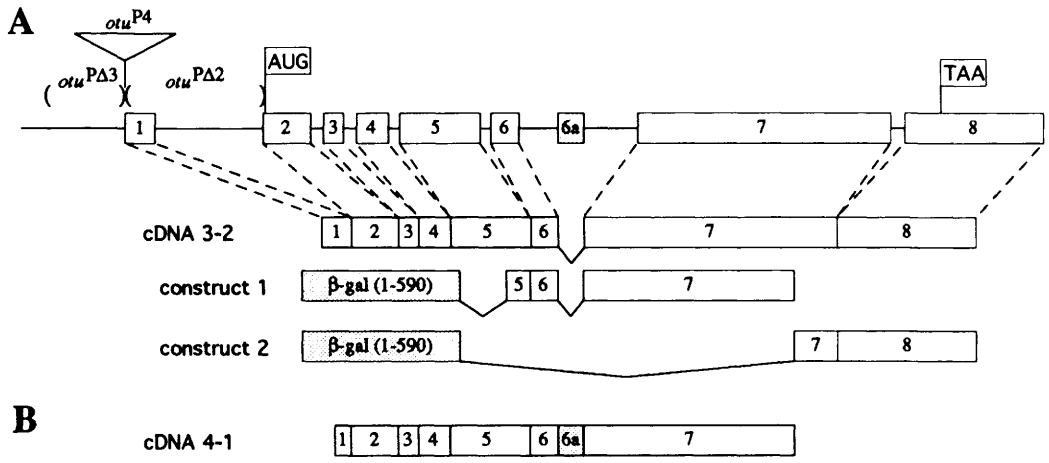

Figure 1. The structures of *otu* cDNAs and fusion proteins. (*A*) The *otu* gene structure with translation initiation and termination sites indicated is shown *above* the schematic exon structure of cDNA 3-2. Approximate locations of lesions from three P-element-induced or -derived mutations are shown at the 5′ end of the *otu* gene. The coding sequences of the *otu* gene ligated into the pWR590 expression vector are identified in constructs 1 and 2. (*B*) Schematic exon structure of cDNA 4-1. Differences between cDNA 4-1 and cDNA 3-2 include the lack of 68 nucleotides from cDNA 3-2 at the 5′ end of cDNA 4-1, the truncation of cDNA 4-1 at an internal *Eco*RI site of cDNA 3-2, and the addition of an alternate exon (6a) in cDNA 4-1 between exons 6 and 7 of cDNA 3-2.

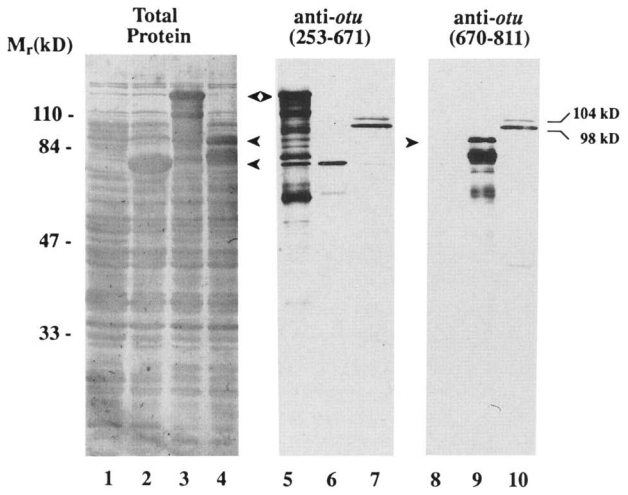

Figure 2. Analysis of the specificity of two anti-*otu* antisera. (Lanes *1–4*) Total protein staining of *E. coli* extracts after fractionation by SDS-PAGE and transfer to nitrocellulose. The positions of the proteins expressed from the original expression vector (lane *2*, 80 kD), and the two fusion constructs: *lacZ–otu*(253–671) (lane *3*, 140 kD) and *lacZ–otu*(670–811) (lane *4*, 90 kD) are indicated by arrowheads. (Lane *1*) An extract of the parent *E. coli* strain (MV1184) without an expression vector; (lanes *5–7*; *8–10*) Equivalent blots of extracts from *E. coli* expressing *lacZ–otu*(253–671) (lanes *5*, *8*), *lacZ–otu*(670–811) (lanes *6*, *9*), or 10 μg of crude ovary extract from Canton-S flies (lanes *7*, *10*). Lanes *5–7* and *8–10* were incubated with anti-*otu*(253–671) and anti-*otu*(670–811) antisera, respectively. The immunostaining proteins below the intact fusion proteins (lanes *5*, *9*) appear to be degradation products of the fusion proteins. Two proteins from Canton-S ovary extracts (at 104 and 98 kD) immunostain with both antisera. The light immunostaining at ~45 kD (lane *10*) appears to be nonspecific staining of the highly abundant vitellogenin proteins from the ovary extracts. The positions of molecular mass markers are shown at *left*.

extracts prepared from *Drosophila* ovaries. In addition to recognizing the 140-kD fusion protein generated from construct 1 (Fig. 2, lane 5), anti-*otu*(253–671) antiserum cross-reacts with an ~80-kD *E. coli* protein and a protein of similar size in ovary extracts (Fig. 2, lanes 6,7); however, as expected, this antiserum does not cross-react with the 90-kD fusion protein generated from construct 2 (Fig. 2, lane 6). Anti-*otu*(670–811) antiserum recognizes the 90-kD fusion protein and does not cross-react with the 140-kD fusion protein (Fig. 2, lanes 8,9). Both antisera recognize two proteins with apparent molecular masses of 98 and 104 kD in crude ovary extracts from wild-type (Canton-S) flies (Fig. 2, lanes 7,10). The apparent mobility of the 98-kD protein is in reasonable agreement with the calculated molecular mass from the amino acid sequence (92.6 kD), assuming that the high proline content of the *otu* protein (12%) reduces mobility (Carroll and Scott 1985; Gaul et al. 1987; Driever and Nüsslein-Volhard 1988; Prost et al. 1988).

In support of these results an additional cDNA clone (4-1) was isolated and sequenced that begins 68 nucleotides downstream from the 5′ end of cDNA 3-2, and extends 3′ to the internal *Eco*RI restriction site of cDNA 3-2 (Steinhauer et al. 1989; Fig. 1B). This cDNA does not contain a poly(A) tract, and its termination at the *Eco*RI restriction site is probably a result of incomplete methylation of the cDNAs during the construction of the library.

The sequence of cDNA 4-1 revealed an additional exon (6a) located between the sixth and seventh exons of previously identified cDNAs (Champe and Laird 1989; Steinhauer et al. 1989). The additional 126-bp exon extends from nucleotide 2780 to 2905 of the *otu* genomic sequence (Figs. 1 and 3). Inclusion of this exon does not disrupt the translational reading frame and results in the addition of 42 amino acids (Fig. 3, 1A–42A) to the 811-amino-acid *otu* isoform (Steinhauer et al. 1989). The peptide translated from this additional exon contains 33% charged residues and maintains the hydrophilic character of the rest of the protein. If the transcript used to generate cDNA 4-1 was equivalent to cDNA 3-2 in the 3′ region beyond the *Eco*RI restriction site, then the calculated molecular mass of the protein (97.4 kD) is in reasonable agreement with the mobility of the 104-kD isoform observed in Western blots, with the assumption that proline content affects mobility.

Further support for two isoforms is the identification of a molecular lesion at the splice acceptor site for the alternate exon in an *otu* mutant allele that accumulates the 98-kD isoform only in ovary extracts (see below). These data suggest that two proteins are derived from the *otu* gene and that the 98-kD protein is considerably more abundant than the 104-kD polypeptide in normal ovary extracts.

Several otu *mutants exhibit alterations in the expression and/or size of* otu *proteins*

We wished to know whether any of the ovarian pathologies of *otu* mutants could be correlated with specific alterations in expression of the two *otu* isoforms. The expression of *otu* proteins in selected alleles was examined by Western blot (see below). This analysis led us to sequence specific genomic regions of four *otu* mutants. The two ONC mutants otu^{11} and otu^{13} were sequenced across the alternate exon and because these mutations were induced in the same parental chromosome, sequence differences between these two alleles should identify mutations rather than background polymorphisms. A 408-bp genomic fragment of otu^{11} and otu^{13} that includes the alternate exon (Fig. 3, nucleotides 2643–3050) was amplified by polymerase chain reaction (PCR), and the amplified DNA was sequenced. Genomic sequence of otu^{13} indicated a G → A base substitution at nucleotide 2779 (Fig. 3). This transition alters the 3′-splice acceptor site adjacent to the 5′ end of the alternate exon by converting the invariant AG dinucleotide, required for splice acceptor site function, to AA. The genomic sequence of otu^{11} contained a G → A base substitution at nucleotide 2793, which converts the cysteine at

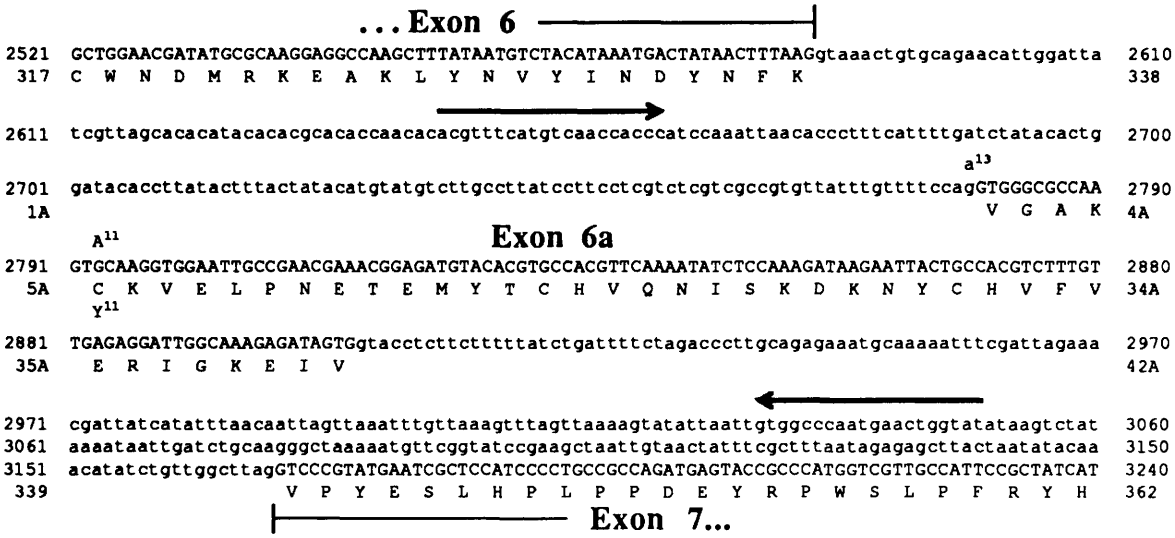

Figure 3. The nucleotide and amino acid sequence of the region that includes the alternate exon of the *otu* gene. The location of the alternate exon of cDNA 4-1, between exons 6 and 7 of the transcript reported previously, is identified within a portion of the *otu* genomic sequence (Steinhauer et al. 1989). The intron sequences are in lowercase and the alternate exon amino acids are identified as 1A–42A. The location of the primers used to perform PCR amplification on the genomic fragments of otu^{11} and otu^{13} across the alternate exon are indicated by arrows. The point mutation of otu^{11} is at nucleotide 2793 (A^{11}) and converts the wild-type cysteine to tyrosine (Y^{11}). The mutation within the otu^{13} allele is at nucleotide 2779 (a^{13}), which disrupts the splice acceptor site for the alternate exon.

amino acid 5A to tyrosine (Fig. 3). A third ONC mutant ($otu^{P\Delta 3}$) is known to have a deletion of ~450 bp upstream of the cDNA start site but has an unaltered coding region (G. Sass et al., in prep.; Fig. 1A).

Of the four ONC mutants examined by Western blot, three (otu^{11}, otu^{3} and $otu^{P\Delta 3}$; Fig. 4, lanes 2, 4, 5) accumulate higher proportions of the larger protein, although the absolute amount of both isoforms is reduced dramatically in two of these mutants (Fig. 4, lanes 4, 5). In the case of $otu^{P\Delta 3}$ the 98-kD isoform is either not expressed or is expressed below the level of detectability. In contrast, the ONC allele otu^{13} (Fig. 4, lane 3) displays nearly wild-type levels of protein but does not accumulate detectable levels of the 104-kD isoform. The absence of the larger isoform is expected because of the splice site mutation at the alternate exon of otu^{13}. These data suggest that ONC mutants are correlated with reduced amounts of the 98-kD isoform with respect to the normal abundance of this isoform in wild-type ovaries.

As with otu^{11} and otu^{13} two DIF alleles otu^{5} and otu^{14} were sequenced within specific regions of the *otu* gene. Because both otu^{5} and otu^{14} accumulate smaller proteins, it seemed likely that these alleles contained nonsense mutations. On the basis of sizes of the truncated proteins in otu^{5} and otu^{14} extracts, an estimate was made of the region within the *otu* gene where premature translation termination signals might be located. Fragments with 219 bp of genomic DNA (nucleotides 3947–4166; Steinhauer et al. 1989) from otu^{5} and otu^{14} were PCR amplified, cloned, and sequenced. Sequences of both mutants contained C → T base substitutions that created stop codons in exon 7, after residue 621 of otu^{5} and residue 655 of otu^{14} (numbered with respect to the 98-kD isoform).

Antiserum that recognizes the carboxy-terminal region of *otu* proteins does not recognize *otu* proteins in

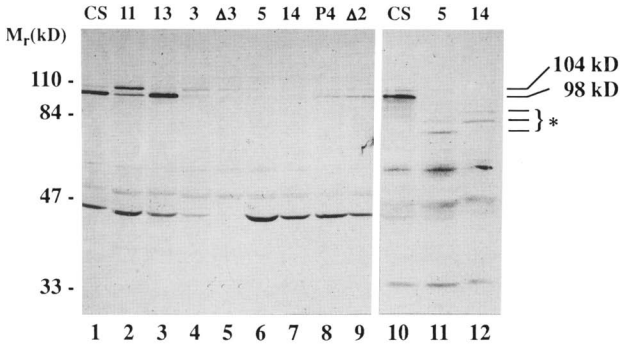

Figure 4. Western analysis of *otu* mutants. Eight mutants were analyzed, four ONC alleles [otu^{11} (lane *2*), otu^{13} (lane *3*), otu^{3} (lane *4*), $otu^{P\Delta 3}$ (lane *5*)], and four DIF alleles [otu^{5} (lanes *6* and *11*), otu^{14} (lanes *7* and *12*), otu^{P4} (lane *8*), $otu^{P\Delta 2}$ (lane *9*)]. A 20-μg aliquot of ovary extract was loaded for each mutant, except for otu^{5} where 40 μg was loaded, and 10 μg of wild-type (Canton-S) ovary extract was loaded in lanes *1* and *10*. Lanes *1–9* were incubated with anti-*otu*(670–811) antiserum; lanes *10–12* were incubated with anti-*otu*(253–671) antiserum. The two *otu* protein isoforms identified in Fig. 2 are indicated (104 and 98 kD), and truncated forms of these proteins from the otu^{5} and otu^{14} alleles are identified by the asterisk (*). Note that these truncated forms are not recognized by the anti-*otu*(670–811) antiserum (lanes *6*, *7*). The positions of molecular mass markers are shown at *left*.

extracts derived from otu^5 and otu^{14} (Fig. 4, lanes 6, 7). However, in extracts from both mutants, antiserum that recognizes the central portion of the *otu* proteins (amino acids 253–671) immunostains two proteins with lower molecular masses than the native *otu* proteins. In otu^5 extracts, 82- and 76-kD polypeptides were detected (Fig. 4, lane 11), whereas in otu^{14} extracts, 86- and 81-kD polypeptides were observed (Fig. 4, lane 12). Calculated molecular masses for the two isoforms are 77.2 and 72.3 kD for otu^5, and 80.6 and 75.8 kD for otu^{14}. These calculated sizes are consistent with the respective masses observed, again with the assumption that proline content affects mobility. Two other DIF mutants, otu^{P4} and $otu^{P\Delta 2}$ (Fig. 4, lanes 8, 9), exhibit the same sized *otu* polypeptides as wild-type flies but at considerably reduced levels. In contrast to the ONC mutants, DIF mutants appear to maintain a more nearly wild-type ratio of the two isoforms with respect to each other.

The truncated proteins of otu^5 and otu^{14} are capable of promoting the early stages of oogenesis, suggesting that 190 amino acids of the carboxyl terminus are not required for proper cyst formation or differentiation. Inability of these mutants to complete oogenesis may be the result of a loss of function associated with the carboxy-terminal domains but could also result from low protein levels as seen in the Western blot, a result of reduced stability of the truncated proteins. Table 1 summarizes the phenotypes and molecular lesions associated with the *otu* alleles examined.

Fertile heteroallelic combinations alter otu *protein expression*

Although most heteroallelic combinations of *otu* yield intermediate phenotypes, the two ONC alleles that express relatively high levels of *otu* protein (otu^{11} and otu^{13}) complement several DIF alleles to fertility. Most of these transheterozygotes have ovaries that contain substantial numbers of tumorous chambers or chambers lacking oocytes, but the chambers that form properly complete development and produce fertile eggs. The exception is the otu^{11}/otu^{14} heterozygotes, which have nearly normal ovarian morphology (Storto and King 1987). Using the DIF alleles otu^5 and otu^{14} and the anti-*otu*(670–811) antiserum that does not recognize the truncated proteins from these alleles, we examined the effects of these DIF alleles on the accumulation of *otu* proteins expressed from otu^{11} and otu^{13} alleles in transheterozygotes.

Heteroallelic combinations of otu^5 and otu^{14} with otu^{11} alter the ratio of the accumulated levels of the two protein isoforms generated from the otu^{11} allele. Whereas otu^{11} homozygotes exhibit nearly equal or greater amounts of the 104-kD isoform in comparison to the smaller isoform (Fig. 5, lane 2; Fig. 4, lane 2), heterozygotes (otu^5/otu^{11} and otu^{14}/otu^{11}) accumulate levels of the two isoforms at nearly wild-type ratios in which the 98-kD isoform is predominant (Fig. 5, lanes 3–6). No change in accumulation of *otu* protein isoforms is observed in heteroallelic combinations of otu^{13} with otu^5 and otu^{14} (Fig. 5, lanes 9–12). This result is as expected because of the splice site mutation at the alternate exon of otu^{13}. These results suggest that the relative ratio of *otu* isoforms expressed from the otu^{11} allele is a function of the ovarian phenotype and that the high level of the 104-kD isoform expressed in homozygotes is a result of the large percentage of tumorous chambers in these ovaries.

Localization of otu *protein in Canton-S and mutant alleles*

We examined the temporal and spatial distribution of *otu* proteins in wild-type and *otu* mutant ovary tissue sections by immunocytochemistry. Immunostaining was evident in cytoplasm of cystocytes, nurse cells, and oocytes, but no *otu* protein was detected in nuclei or follicle cells. Intense immunostaining is present in ger-

Table 1. *Selected alleles of the* otu *locus and their associated lesions*

Allele	Class	Ovarian phenotypes		Molecular lesion
		homozygotes	hemizygotes	
otu^{11}	ONC	tumorous	tumorous	G → A substitution at position 2793; Cys → Tyr transition at position 5A of alternate exon
otu^{13}	ONC	tumorous	tumorous	G → A substitution at position 2779; alters the splice acceptor at the 5′ end of exon 6a
otu^3	ONC	tumorous	quiescent	unknown
$otu^{P\Delta 3}$	ONC	tumorous	quiescent	≈450-bp deletion 5′ of cDNA 3-2 start site (Fig. 1A)
otu^5	DIF	differentiated	quiescent	C → T substitution at position 4018; 190-amino-acid truncation after residue 621
otu^{14}	DIF	differentiated	differentiated	C → T substitution at position 4120; 156-amino-acid truncation after residue 655
otu^{P4}	DIF	differentiated	ND	≈500-bp insertion near cDNA 3-2 start site (Fig. 1A)
$otu^{P\Delta 2}$	DIF	differentiated	tumorous	≈700-bp deletion 3′ of cDNA 3-2 start site (Fig. 1A); deletes most of the 5′-untranslated leader sequence

Position numbers are as in Fig. 3 and Steinhauer et al. (1989). Residue numbers for the truncated proteins are with respect to the 98-kD isoform. (ND) Not determined.

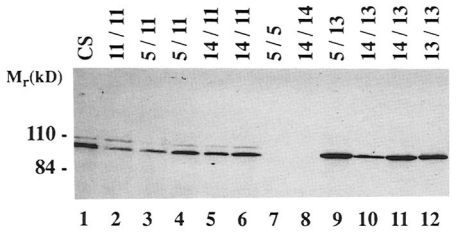

Figure 5. Western analysis of heteroallelic combinations of *otu* mutant alleles. Heteroallelic combinations were made of two ONC mutants (*otu*^{11} and *otu*^{13}) with each of two DIF mutants (*otu*^{5} and *otu*^{14}). The genotypes of the flies from which the ovary extracts were made are indicated *above* each lane. Only the wild-type Canton-S (CS), *otu*^{11}, and *otu*^{13} alleles express *otu* proteins, which can be recognized by the antiserum used to probe this Western blot. Lane *1* has 10 μg of ovary extract loaded; the other lanes have either 20 μg (lanes *2,3,5,7,8,10,12*) or 40-μg (lanes *4, 6, 9, 11*) loaded. The 40 μg loadings compensate for heterozygotes with only one allele that expresses recognizable protein.

maria of wild-type ovaries, and staining intensity remains constant or decreases slightly through stage 4 (Fig. 6A). From stage 5 or 6, staining intensity increases steadily to a plateau at stages 9–10B. Staining is lost in nurse cells gradually and follows the degeneration of these cells. In contrast, *otu* protein in oocytes is degraded beyond detectability during stage 11 (Fig. 6B), a stage that lasts only 0.4 hr (David and Merle 1968; Mahowald and Kambysellis 1980). Control tissues incubated with antisera, in which *otu*-specific antibodies had been removed by passing the sera over a fusion protein-affinity column, displayed very low levels of immunostaining (Fig. 6C).

Results of an immunostaining analysis of *otu* proteins in *otu*^{11}, *otu*^{13}, and *otu*^{14} were in agreement with the Western analysis concerning levels of protein accumulation. Staining was severely reduced in the DIF mutant *otu*^{14}, while two ONC mutants, *otu*^{11} and *otu*^{13}, displayed considerable staining (Fig. 6D–F). Furthermore the ONC mutants exhibit more intense staining in differentiated chambers than in tumorous chambers (Fig. 6D, E). This may reflect greater expression from polyploid nuclei of differentiated cystocytes or may be the result of smaller cytoplasmic volume in tumorous chambers. Germaria of *otu*^{14} ovaries immunostain, but there is no increase in the levels of staining as oogenesis progresses and staining is very weak in later stages (Fig. 6F). This weak staining may indicate an instability of the truncated proteins expressed from the *otu*^{14} allele.

Discussion

Alternative splicing of otu *pre-mRNA generates two protein isoforms upon translation*

We have described a cDNA from the *otu* locus that contains an extra exon between the sixth and seventh exons of the transcript reported previously (Steinhauer et al. 1989). Antibodies raised against fusion proteins generated with two different regions of *otu*-coding sequences each recognize two protein isoforms of sizes that correspond to the molecular masses predicted by the conceptual translation of the two cDNAs. Western analysis showed that both isoforms were altered in *otu* mutants, either in mobility or relative abundance. Particularly convincing evidence for the relevance of both bands is the absence of the larger isoform in *otu*^{13} and truncation of both isoforms in *otu*^{5} and *otu*^{14}. Each of these alterations has been correlated with a point mutation that disrupts a splice junction of the alternate exon (*otu*^{13}) or creates a nonsense mutation (*otu*^{5} and *otu*^{14}). The splice site mutation in *otu*^{13} prevents appropriate splicing of the alternate exon that results in the absence of the larger isoform in *otu*^{13} ovary extracts. Although these three alleles have not been sequenced across the entire *otu*-coding region, the correlation of a specific point mutation with a predicted observable change in protein expression on Western blots is strong evidence that the identified lesions are responsible for the mutant phenotypes of these alleles. We conclude that two protein isoforms are derived from *otu* by an alternative splicing mechanism.

A shift in protein expression may coincide with cystocyte differentiation

Our results show a shift in accumulation of one *otu* protein isoform over the other that may coincide with differentiation of the germ cells. If a correlation exists between the state of differentiation and the expression of a specific *otu* isoform, then the ratio of the two isoforms in an extract will be a function of the degree of differentiation of germ cells within the ovary. Therefore, amounts of a specific isoform in extracts from ovaries with varying degrees of differentiation cannot be directly compared. For instance, ovary extracts from DIF mutants (mostly differentiated germ cells), which may be expressing greater amounts of the 104-kD isoform in predifferentiated germ cells than ONC mutants (mostly undifferentiated germ cells), may still accumulate less of this isoform because of the greater percentage of predifferentiated germ cells in ONC mutants. Therefore, only the total level of expression of both isoforms and the relative ratio of the two isoforms can be compared between phenotypes. Furthermore, the ratio of the isoforms in a specific mutant will not be constant because of variability in the degree of differentiation in different extracts. For instance, the two different extracts of *otu*^{11} ovaries (Fig. 4, lane 2; Fig. 5, lane 2) show varying ratios of the two isoforms, which presumably reflects varying degrees of differentiation in these ovary preparations. We have shown that ovary extracts from *otu* mutants, characterized by greater percentages of undifferentiated germ cells within their ovaries than wild-type flies, exhibit correspondingly greater ratios of the 104-kD isoform to the 98-kD isoform, whereas *otu* alleles characterized by more normal percentages of differentiated germ cells within their ovaries showed more normal ratios of the two isoforms. Moreover, when we experimentally alter

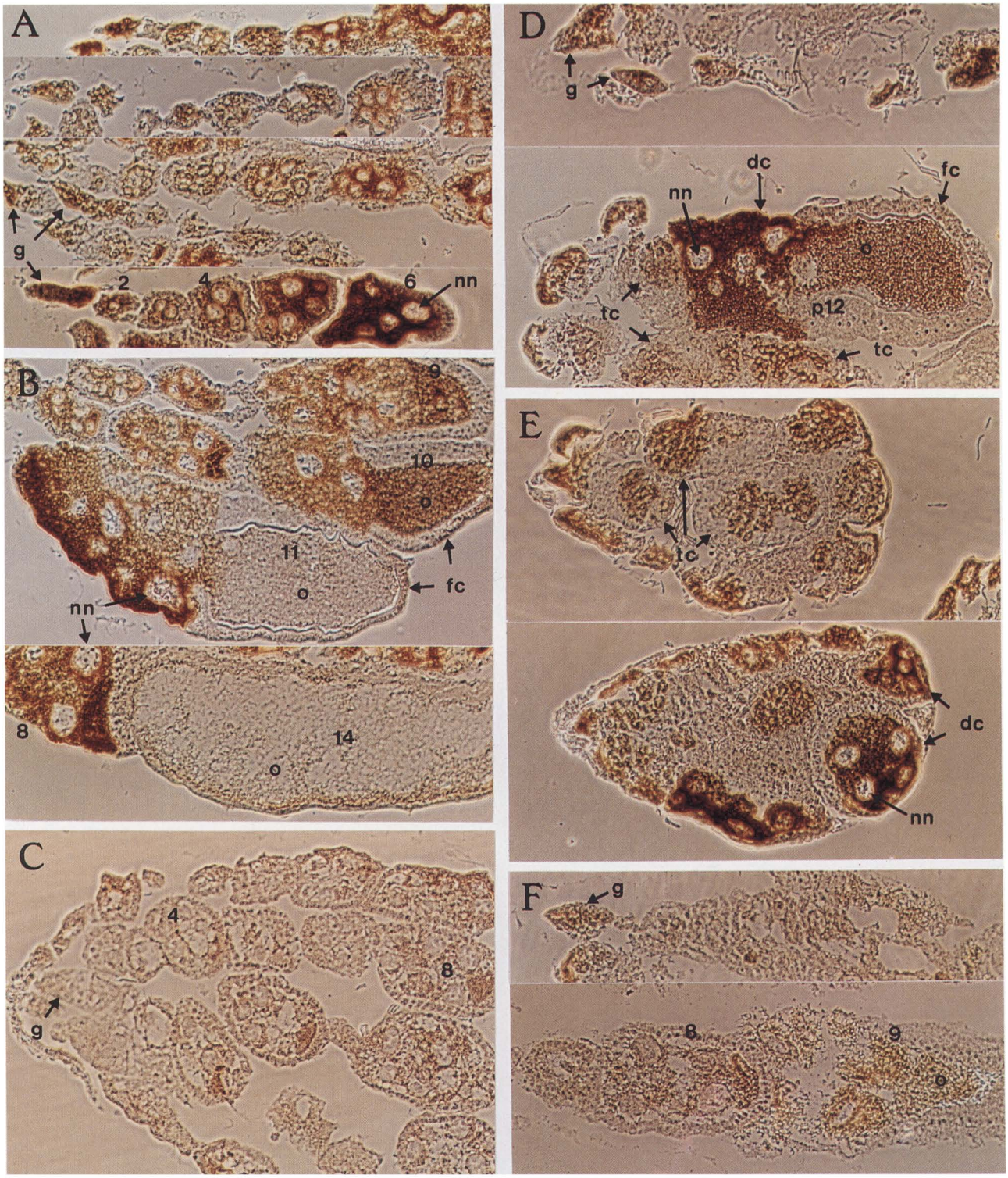

Figure 6. In situ localization of *otu* proteins in wild-type (Canton-S) and *otu* mutant ovaries. Frozen sections (6 μm) were incubated with anti-*otu*(670–811) antiserum (*A*,*B*,*D*,*E*), control antiserum (*C*), or anti-*otu*(253–671) antiserum (*F*). Localization of *otu* proteins was accomplished by the avidin–biotin peroxidase complex technique. (*dc*) Differentiated egg chamber; (*fc*) follicle cells; (*g*) germarium; (*nn*) nurse cell nuclei; (*o*) oocyte; (*p12*) psuedo-12-stage egg chamber; (*tc*) tumorous chamber. Numbers within egg chambers represent the developmental stage of the egg chamber. (*A–C*) Sections from wild-type (Canton-S) ovaries exhibit germarial staining and strong cytoplasmic staining in nurse cells and oocytes. Oocyte staining has disappeared by stage 11 (*B*). (*C*) Most of the immunostaining is removed by passing anti-*otu*(670–811) antiserum over a *lacZ–otu*(670–811) affinity column prior to incubation with the sections. (*D*) Sections from otu^{11} ovaries exhibit moderate staining in germaria and tumorous chambers and strong staining in differentiated egg chambers. (*E*) Immunostaining in otu^{13} ovaries is similar to that of otu^{11} ovaries. (*F*) Sections from otu^{14} ovaries exhibited light germarial staining, but no significant accumulation of *otu* proteins is seen in later stages of oogenesis as is seen in wild-type ovaries.

the degree of differentiation of the ovaries in which an otu^{11} allele is present through heteroallelic combinations, a shift in the ratio of the two isoforms results (i.e., the pattern of expression from the otu^{11} allele is shifted from a predominance of the 104-kD isoform in homozygotes to a predominance of the 98-kD isoform in otu^{11}/otu^{5} and otu^{11}/otu^{14} heterozygotes).

Although it appears likely, we cannot conclude that normal undifferentiated germ cells express only the 104-kD isoform, because ovaries of most ONC alleles contain both differentiated and undifferentiated chambers. However, the ONC allele $otu^{P\Delta 3}$, which has unaltered coding sequences (Fig. 1 and Table 1) and contains only undifferentiated germ cells (G.Sass, unpubl.), does not accumulate detectable levels of the 98-kD isoform. The accumulated data suggest that differentiation of cystocytes into nurse cells and an oocyte alters the splicing pathway of *otu* pre-mRNA, shunting splicing toward removal of the alternate exon. This is not to say that expression of the 98-kD isoform brings about differentiation of cystocytes but is a result of that differentiation. Alternatively, differentiation could affect the stability of one mRNA or protein species more than the other.

A model for otu *expression*

It has been proposed that the *otu* gene product is required in increasing amounts throughout oogenesis and that different classes of *otu* mutants reflect phenocritical thresholds of functional *otu* protein expression (King and Riley 1982; King et al. 1986). The fact that heteroallelic combinations of some ONC alleles with some DIF alleles yield fertile flies rather than flies with intermediate ovarian pathologies suggests that a second *otu* product exists and that each complementing allele provides one of the required functions (Storto and King 1987). It is remarkable that the hypothesis developed by King and his collegues from genetic and morphological analyses should, for the most part, predict observed molecular data so closely.

The three developmental classes (QUI, ONC, and DIF) that categorize *otu* phenotypes highlight three stages of oogenesis where *otu* gene products appear to have a major function: stem cell proliferation, control of germ cell divisions and differentiation, and oocyte development. The first two stages require only low levels of *otu* expression as evidenced by the reduced levels of *otu* proteins in two of the ONC mutants and all of the DIF mutants examined. Furthermore, the threshold of expression that separates the ONC and DIF phenotypes appears to be very narrow because among mutants that have unaltered coding regions, DIF mutants accumulate only slightly greater amounts of *otu* products than ONC mutants. Several observations lead us to conclude that later stages of oogenesis require greater accumulation of *otu* protein for normal oocyte development. First, results from an in situ analysis suggest that *otu* proteins accumulate to high levels in nurse cells of stage 11 egg chambers. Second, all DIF mutants examined accumulate much less protein than wild-type flies. The molecular lesions in otu^{5} and otu^{14} result in truncated *otu* proteins; and by immunocytochemical analysis (otu^{14}), the truncations appear primarily to destabilize the proteins and prevent their accumulation in later stages of oogenesis. Finally, heteroallelic crosses of otu^{14} with ONC alleles are fertile when the ONC alleles express high levels of *otu* proteins (otu^{11} and otu^{13}), but are sterile when the ONC alleles express low levels of *otu* proteins (otu^{3} and $otu^{P\Delta 3}$). Thus, the termination of oogenesis around stage 12 in otu^{14} mutants can be overcome by providing a stable and abundant source of the 98-kD isoform.

We have suggested that a shift in expression coincides with differentiation of germ cells, but is there a requirement for a specific isoform at any specific stage of oogenesis? The control of cyst formation and differentiation appears to be sensitive to which *otu* isoform is expressed, as suggested by the observations outlined here. (1) Two ONC mutants otu^{11} and otu^{13} accumulate high levels of *otu* protein and yet give rise to tumorous ovaries, a more severe ovarian pathology than that of the DIF mutants examined, which accumulate much less *otu* protein. (2) Point mutations, which affect the alternate exon (6a) and, hence, the 104-kD isoform, have been identified in both otu^{11} and otu^{13}. (3) Truncated *otu* proteins are expressed from two DIF alleles otu^{5} and otu^{14}, which presumably have normal alternate exons, yet these truncations have little discernible effect on cyst formation or differentiation. Moreover, otu^{11} and otu^{13} presumably produce perfectly functional 98-kD isoform and generate fertile flies when crossed with otu^{5} or otu^{14}, which can provide *otu* function through differentiation. These data in conjunction with the evidence that the 104-kD isoform is the predominant *otu* protein in undifferentiated cystocytes suggest that this isoform plays an important role in controlling the early mitotic divisions of oogenesis. Although the larger isoform appears to be important for controlling these early divisions and generating normal cysts, it is not absolutely required for cystocyte differentiation, because otu^{13} lacks this isoform entirely and yet produces some differentiated chambers. Perhaps high levels of the 98-kD isoform can promote cystocyte differentiation inefficiently.

Our present hypothesis is that the 104-kD isoform is expressed early in oogenesis and is required for proper control of germ cell divisions. The onset of differentiation results in an alternative splice such that the 98-kD isoform is expressed in stages subsequent to differentiation and that this isoform accumulates progressively in germ cell cytoplasm through stage 11, except in oocytes where it is rapidly degraded at the beginning of stage 11. These latter stages of oogenesis presumably require high levels of *otu* protein, as low levels result in the termination of development.

How might otu *function?*

Proteins from *otu* appear to play an important role in at least three different processes of oogenesis: stem cell proliferation, control of germ cell divisions, and degeneration and collapse of the nurse cells. In light of the

distribution of *otu* protein in ovaries (i.e., in germ-cell cytoplasm) we think the most likely function of *otu* is in controlling cytoskeletal reorganizations. The high level of *otu* protein in ovaries suggests the possibility that these proteins are integral components of specific cytoskeletal structures. However, *otu* proteins could also affect cytoskeletal reorganization by a number of alternatives.

Two studies support the idea that *otu* proteins perform a cytoskeletal role. The characteristic branched structure of 16-cell cysts is thought to be generated by a structure known as a polyfusome, which occupies the ring canals of the cyst (Maziarski 1913; Koch and King 1969; Mahowald and Strassheim 1970; Mahowald 1971; Telfer 1975; King and Storto 1988). Examination by electron microscopy and reconstruction of serial sections of germaria from the ONC mutant otu^1 revealed that this mutant could not sustain a series of arrested cleavages and that its fusomal material contained ultrastructural differences from normal polyfusomes (Storto and King 1989). It was suggested that *otu* gene products are involved in the organization and maintenance of ring canals through stabilization of the polyfusome, and if differentiation of cystocytes is linked to appropriate cyst formation then a disruption of the polyfusome could result in continued cell division and a tumorous phenotype. Nurse cell cytoplasmic transport is arrested in the DIF mutant otu^7, and this mutant lacks a network of actin microfilaments in nurse cells (Storto and King 1988), which are proposed to provide contractile forces that transport nurse cell cytoplasm into the oocyte through the ring canals (Gutzeit 1986). Interestingly, rapid loss of *otu* immunostaining in oocytes of normal egg chambers is coincident with development of actin filament networks in nurse cells and the cytoplasmic transport process. If *otu* gene products perform a role in organizing the microfilament network perhaps degradation of *otu* protein in oocytes is required to prevent similar networks from forming in oocytes.

Although these cytoskeletal anomalies cannot account for the entire spectrum of *otu* mutant phenotypes, they provide insight into the function of *otu* proteins during oogenesis and a direction for studies of protein interactions with *otu* gene products.

Materials and methods

Antibody generation and purification

Production of anti-*otu*(253–671) antiserum has been described previously (Steinhauer et al. 1989). Anti-*otu*(670–811) antiserum was produced by inserting a 3′ *Eco*RI restriction fragment of cDNA 3-2 (nucleotides 4161–5177 excluding the intron; Steinhauer et al. 1989) into the pWR590 expression vector (Guo et al. 1984). The *lacZ–otu* fusion construct was used to transform *E. coli* MV1184 cells. The expressed 90-kD fusion protein was partially purified by insoluble aggregation (Williams et al. 1982; Rio et al. 1986) and then gel purified by SDS-PAGE. Protein bands were visualized by Coomassie staining in water, excised, electroeluted, and precipitated with 8 vol of ethanol. Precipitated protein (50–200 μg) was resuspended in a buffer containing 50 mM Tris-HCl (pH 8.0), 0.2% SDS, and 0.3 M NaCl, emulsified in an equal volume of Freund's complete adjuvant, and injected in multiple subcutaneous sites of rabbits. Rabbits were boosted at 3-week intervals with protein prepared as described above, emulsified in an equal volume of Freund's incomplete adjuvant.

Affinity columns were prepared with both fusion proteins by coupling to Affi-gel 10 (1 mg of protein/ml of gel), following the manufacturer's specifications (Bio-Rad). Coupling buffer was 0.1 M $NaHCO_3$ (pH 8.5), 0.3 M NaCl, and when required, 0.2% SDS was included to keep the fusion protein in solution. Addition of SDS in the coupling buffer did not interfere with coupling. High-titer sera were affinity purified on a *lacZ–otu*(670–811) fusion protein-affinity column following removal of antibodies against β-galactosidase on a *lacZ–otu*(253–671) fusion protein column. Loadings, washes, and elutions followed the procedures described by Robbins et al. (1984).

Sequence analysis

cDNA 4-1 was excised from λgt11 (Huynh et al. 1985) by *Eco*RI digestion and inserted into *Eco*RI-digested M13mp8 (Messing 1983). The cDNA consists of two *Eco*RI fragments resulting from what appears to be a single-base change at nucleotide 2516 (Steinhauer et al. 1989), creating an additional *Eco*RI site. Nucleotide sequences were determined by the dideoxy chain-termination method (Sanger et al. 1977) on M13 single-stranded phage templates. The complete sequence of the alternate cDNA was determined on one strand by using oligonucleotide primers designed from the published sequence (Steinhauer et al. 1989). Sequences were assembled and analyzed with the University of Wisconsin Genetics Computer Group programs (Devereux et al. 1984).

Western analysis

Ovaries were dissected from 2- to 6-day-old females that had been fed on yeast paste for 2 days at 18°C. Ovaries were homogenized in buffer containing 50 mM Tris-HCl (pH 7.5), 3 mM EDTA, 1% NP-40, 0.1% SDS, 1 mM *N*-ethylmaleimide, 100 μM leupeptin, 10 μM pepstatin, 3 trypsin inhibitor units (TIU) of aprotinin/ml, and 100 μg/ml PMSF and centrifuged at 13,000*g* for 3 min. Protein concentrations of the supernatants were determined by the method of Bradford (1976). Protein recoveries were typically 5–10 μg/ovary from Canton-S or *otu* DIF alleles and 0.5–1 μg/ovary from *otu* ONC alleles.

Samples containing 10–20 μg of protein were mixed with equal volumes of 2× sample buffer (Laemmli 1970) and fractionated on 10% SDS–polyacrylamide gels (1.5 mm). Proteins were blotted to nitrocellulose overnight by electrophoretic transfer (Towbin et al. 1979). Efficiency of transfer was estimated by transfer of prestained molecular mass markers (Bio-Rad). Blots were blocked for 1 hr with 1% BSA (Promega) in TBST [10 mM Tris-HCl (pH 8.0), 150 mM NaCl, 0.1% Tween-20] followed by primary antibody incubation in TBST. Incubation times varied with the antibodies used [anti-*otu*(253–671), 1 hr; anti-*otu*(670–811), 3 hr]. After washing four times for 10 min each in TBST, blots were incubated with alkaline phosphatase-conjugated goat anti-rabbit secondary antibody in TBST for 1 hr (Boehringer Mannheim, 1 : 5000). Blots were washed four times for 10 min each in TBST and developed with BCIP and nitroblue tetrazolium (Bio-Rad) following the manufacturer's specifications.

PCR amplification

Genomic DNA for PCR amplification was prepared from mutant flies by mashing three flies with a toothpick in 50 μl of a

buffer containing 10 mM Tris-HCl (pH 8.2), 1 mM EDTA, 25 mM NaCl, and 200 μg/ml of proteinase K. Homogenates were heated to 95°C for 15 min and, after addition of 2 μl of 10 mg/ml PMSF, reheated to 65°C for an additional 15 min. Homogenates were then centrifuged to pellet the debris, and the supernatant was removed. A 10-μl aliquot of this supernatant was used in each PCR reaction.

PCR (Saiki et al. 1988) was performed with the GeneAmp kit (Perkin-Elmer Cetus) following the manufacturer's specifications. Reactions were cycled 30 times (94°C for 1 min, 55°C for 1 min, 70°C for 1 min), and resulting fragments were digested with *Eco*RI and *Hin*dIII, gel purified, and inserted into *Eco*RI/*Hin*dIII-digested M13mp8 and M13mp9. Primers for amplifying across the alternate exon were ATCAAGCTT-2643–2662 (Fig. 3) and AGCGAATTC-3050–3031 (Fig. 3), which amplified a 408-bp genomic fragment from otu^{11} and otu^{13}. The primers used to find the nonsense mutations in otu^{5} and otu^{14} were GCTAAGCTT-3947–3966 and 4197–4178 (for sequence, see Steinhauer et al. 1989). In this case, the internal *Eco*RI restriction site just upstream of the 3′ primer, along with the *Hin*dIII site in the 5′ primer, was used to clone the amplified 251-bp genomic fragment. Use of the internal *Eco*RI site resulted in the insertion of 219 bp of genomic DNA from otu^{5} and otu^{14} into *Eco*RI/*Hin*dIII-digested M13mp8 and M13mp9. All sequencing reactions were performed as described above.

Tissue preparation and immunoperoxidase staining

Prior to immunostaining, control antisera were generated by removal of *otu*-specific antibodies on fusion protein-affinity columns. Two hundred microliters of anti-*otu*(670–811) antiserum was loaded onto a *lacZ–otu*(253–671) and a *lacZ–otu*(670–811) affinity column, and washed with 10 ml of PBS containing 1% BSA, and the flowthrough was recycled over the column four times. The final flowthrough from the *lacZ–otu*(253–671) column was the experimental sera, whereas the flowthrough from the *lacZ–otu*(670–811) column served as the control sera. Similarly, 80 μl of anti-*otu*(253–671) antiserum was loaded on affinity columns and processed as described above. Flowthrough from the *lacZ–otu*(670–811) column was the experimental sera, and flowthrough from the *lacZ–otu*(253–671) column was the control sera.

Ovaries were dissected from 2- to 6-day-old females that had been fed on yeast paste for 2 days at 18°C. Ovaries were frozen directly in optimally controlled temperature (OCT) compound (Miles, Inc.) and sectioned (6 μm) on a cryotome. Sections were mounted on glass slides coated with poly-L-lysine and air-dried at room temperature. Sections were fixed with formalin for 30 min, washed twice for 5 min in PBS [10 mM sodium phosphate (pH 7.4), 150 mM NaCl], and treated with 1% H_2O_2 in PBS for 10 min. After two rinses with PBS and a 10-min incubation with 2% lamb serum in PBS, sections were incubated for 24–48 hr at 4°C with dilutions [anti-*otu*(253–671) (1 : 40); anti-*otu*(670–811) (1 : 4)] of the experimental and the control antisera in PBS containing 1% BSA. Immunoreactivity was localized by the avidin–biotin peroxidase complex technique (Hsu et al. 1981), using diaminobenzidine for formation of the reaction product.

Acknowledgments

This work is dedicated to the memory of Laura J. Kalfayan who died of cancer on May 9, 1990. I thank Chris Ingraham for technical guidance on immunocytochemistry, and Allen Comer, Georgette Sass, and Rosemary Walsh for valuable discussions. I thank Bob King, Mimi Sander, Lillie Searles, Ron Swanstrom, Alan Spradling, and Bob Voelker for constructive criticism of the manuscript. This work was funded by grant NP-657 from the American Cancer Society.

The publication costs of this article were defrayed in part by payment of page charges. This article must therefore be hereby marked "advertisement" in accordance with 18 USC section 1734 solely to indicate this fact.

References

Bradford, M. 1976. A rapid and sensitive method for the quantitation of microgram quantities of protein utilizing the principle of protein-dye binding. *Anal. Biochem.* **72:** 248–254.

Brown, E.H. and R.C. King. 1964. Studies on events resulting in formation of an egg chamber in *Drosophila melanogaster*. *Growth* **28:** 41–81.

Carroll, S.B. and M.P. Scott. 1985. Localization of the *fushi tarazu* protein during *Drosophila* embryogenesis. *Cell* **43:** 47–57.

Champe, M.A. and C.D. Laird. 1989. Nucleotide sequence of a cDNA from the putative *ovarian tumor* locus of *Drosophila melanogaster*. *Nucleic Acids Res.* **17:** 3304.

Cummings, M.R. and R.C. King. 1969. The cytology of the vitellogenic stages of oogenesis in *Drosophila melanogaster*. I. General staging characteristics. *J. Morphol.* **128:** 427–442.

David, J. and J. Merle. 1968. A re-evaluation of the duration of egg chamber stages in oogenesis of *Drosophila melanogaster*. *Drosophila Inform Serv.* **43:** 122–123.

Devereux, J., P. Haeberli, and O. Smithies. 1984. A comprehensive set of sequence analysis programs for the VAX. *Nucleic Acids Res.* **12:** 387–395.

Digan, M.E. 1980. "A genetic analysis of chorion morphogenesis in *Drosophila* melanogaster." Ph.D. thesis, Indiana University, Bloomington, IN.

Driever, W. and C. Nüsslein-Volhard. 1988. A gradient of *bicoid* protein in *Drosophila* embryos. *Cell* **54:** 263–269.

Gans, M., C. Audit, and M. Masson. 1975. Isolation and characterization of sex-linked female-sterile mutants in *Drosophila melanogaster*. *Genetics* **81:** 683–704.

Gaul, U., E. Seifert, R. Schuh, and H. Jäckle. 1987. Analysis of *krüpple* protein distribution during early *Drosophila* development reveals posttranslational regulation. *Cell* :639–647.

Guo, L., P.P. Stepien, J.Y. Tso, R. Brousseau, S. Narang, D.Y. Thomas, and R. Wu. 1984. Synthesis of human insulin gene. VIII. Construction of expression vectors for fused proinsulin production in *Escherichia coli*. *Gene* **29:** 251–254.

Gutzeit, H.O. 1986. The role of microfilaments in cytoplasmic streaming in *Drosophila* follicles. *J. Cell Sci.* **80:** 159–169.

Hsu, S.M., L. Raine, and H. Fanger. 1981. Use of avidin-biotin peroxidase complex (ABC) in immunoperoxidase techniques: A comparison between ABC and unlabeled antibody (PAP) procedures. *J. Histochem. Cytochem.* **29:** 577–580.

Huynh, T.V., R.A. Young, and R.W. Davis. 1985. Constructing and screening cDNA libraries in λgt10 and λgt11. In *DNA cloning techniques: A practical approach* (ed. D. Glover), pp. 49–78. IRL Press, Oxford.

Kinderman, N.B. and R.C. King. 1973. Oogenesis in *Drosophila virilis*. I. Interactions between the ring canal rims and the nucleus of the oocyte. *Biol. Bull.* **144:** 331–354.

King, R.C. 1970. *Ovarian development in* Drosophila melanogaster. Academic Press, New York.

———. 1979. Aberrant fusomes in the ovarian cystocytes of the *fs(1)231* mutant of *Drosophila melanogaster* Meigen (Diptera: Drosophilidae). *Int. J. Insect Morphol. Embryol.* **8:** 297–309.

King, R.C. and S.F. Riley. 1982. Ovarian pathologies generated

by various alleles of the *otu* locus in *Drosophila melanogaster*. *Dev. Genet.* **3:** 69–89.

King, R.C. and P.D. Storto. 1988. The role of the *otu* gene in *Drosophila* oogenesis. *BioEssays* **8:** 18–24.

King, R.C., A.C. Rubinson, and R.F. Smith. 1956. Oogenesis in adult *Drosophila melanogaster*. *Growth* **20:** 121–157.

King, R.C., D. Mohler, S.F. Riley, P.D. Storto, and P.S. Nicolazzo. 1986. Complementation between alleles at the *ovarian tumor* locus of *Drosophila melanogaster*. *Dev. Genet.* **7:** 1–20.

Koch, E.A. and R.C. King. 1969. Further studies on the ring canal system of the ovarian cystocytes of *Drosophila melanogaster*. *Z. Zellforsch.* **102:** 129–152.

Laemmli, U.K. 1970. Cleavage of structural proteins during the assembly of the head of bacteriophage T4. *Nature* **227:** 680–685.

Mahowald, A.P. 1971. The formation of ring canals by cell furrows in *Drosophila*. *Z. Zellforsch. Mikrosk. Anat.* **118:** 162–167.

Mahowald, A.P. and J.M. Strassheim. 1970. Intercellular migration of centrioles in the germarium of *Drosophila melanogaster*. An electron microscopic study. *J. Cell Biol.* **45:** 306–320.

Mahowald, A.P. and M.P. Kambysellis. 1980. Oogenesis. In *Genetics and biology of Drosophila* (ed. M. Ashburner and T.R.F. Wright), vol. 2d, pp. 141–224. Academic Press, New York.

Maziarski, S. 1913. Sur la persistance désidus fusariaux pendant les nombreuses générations cellulaires au cours de l'ovogénese de Vespa vulgaris. *L. Arch. Zellforsch.* **10:** 507–532.

Messing, J. 1983. New M13 vectors for cloning. *Methods Enzymol.* **101:** 20–78.

Mohler, J.D. 1977. Developmental genetics of the *Drosophila* egg. I. Identification of 59 sex-linked cistrons with maternal effects on embryonic development. *Genetics* **85:** 259–272.

Mulligan, P.K. and E.M. Rasch. 1985. Determination of DNA content in the nurse and follicle cells from wild-type and mutant *Drosophila melanogaster* by DNA-Fuelgen cytophotometry. *Histochemistry* **82:** 233–247.

Mulligan, P.K., J.D. Mohler, and L.J. Kalfayan. 1988. Molecular localization and developmental expression of the *otu* locus of *Drosophila melanogaster*. *Mol. Cell Biol.* **8:** 1481–1488.

Prost, E., F. Deryckere, C. Roos, M. Haenlin, V. Pantesco, and E. Mohier. 1988. Role of the oocyte nucleus in determination of the dorsoventral polarity of *Drosophila* as revealed by molecular analysis of the K10 gene. *Genes & Dev.* **2:** 891–900.

Rio, D.C., F.A. Laski, and G.M. Rubin. 1986. Identification and immunochemical analysis of biologically active *Drosophila* P element transposase. *Cell* **44:** 21–32.

Robbins, A., W.S. Dynan, A. Greenleaf, and R. Tjian. 1984. Affinity-purified antibody as a probe of RNA polyemerase II subunit structure. *J. Mol. Appl. Genet.* **2:** 343–353.

Saiki, R.K., D.H. Gelfand, S. Stoffel, S.J. Scharf, R. Higuchi, G.T. Horn, K.B. Mullis, and H.A. Erlich. 1988. Primer-directed enzymatic amplification of DNA with a thermostable DNA polymerase. *Science* **239:** 487–491.

Sanger, F., S. Nicklen, and A.R. Coulson. 1977. DNA sequencing with chain-terminating inhibitors. *Proc. Natl. Acad. Sci.* **74:** 5463–5467.

Steinhauer, W.R., R.C. Walsh, and L.J. Kalfayan. 1989. Sequence and structure of the *Drosophila melanogaster ovarian tumor* gene and generation of an antibody specific for the *ovarian tumor* protein. *Mol. Cell. Biol.* **9:** 5726–5732.

Storto, P.D. and R.C. King. 1987. Fertile heteroallelic combinations of mutant alleles of the *otu* locus of *Drosophila melanogaster*. *Wilhelm Roux's Arch. Dev. Biol.* **196:** 210–221.

———. 1988. Multiplicity of functions for the *otu* gene products during *Drosophila* oogenesis. *Dev. Genet.* **9:** 91–120.

———. 1989. The role of polyfusomes in generating branched chains of cystocytes during *Drosophila* oogenesis. *Dev. Genet.* **10:** 70–86.

Telfer, W.H. 1975. Development and physiology of the oocyte-nurse cell syncytium. *Adv. Insect Physiol.* **11:** 223–319.

Towbin, H., T. Staehelin, and J. Gordon. 1979. Electrophoretic transfer of proteins from polyacrylamide gels to nitrocellulose sheets: Procedure and some applications. *Proc. Natl. Acad. Sci.* **76:** 4350–4354.

Williams, D.C., R.M. Van Frank, W.L. Muth, and J.P. Burnett. 1982. Cytoplasmic inclusion bodies in *Escherichia coli* producing biosynthetic human insulin proteins. *Science* **215:** 687–689.

A specific ovarian tumor protein isoform is required for efficient differentiation of germ cells in Drosophila oogenesis.

W R Steinhauer and L J Kalfayan

Genes Dev. 1992, **6:**
Access the most recent version at doi:10.1101/gad.6.2.233